MECHANICAL MASS-SPRING MODEL FOR UNDERSTANDING GLOBULAR MOTION OF PROTEINS

J.-I. Kim

Department of Mechanical Engineering
Korea University
Seoul, Republic of Korea

K. Eom

College of Sport Science
Sungkyunkwan University
Suwon, Republic of Korea

S. Na *

Department of Mechanical Engineering
Korea University
Seoul, Republic of Korea

ABSTRACT

The conformational (structural) change of proteins plays an essential role in their functions. Experiments have been conducted to try to understand the conformational change of proteins, but they have not been successful in providing information on the atomic scale. Simulation methods have been developed to understand the conformational change at an atomic scale in detail. Coarse-grained methods have been developed to calculate protein dynamics with computational efficiency when compared with than all-atom models. A structure-based mass-spring model called the elastic network model (ENM) showed excellent performance in various protein studies. Coarse-grained ENM was modified in various ways to improve the computational efficiency, and consequently to reduce required computational cost for studying the large-scale protein structures. Our previous studies report a modified mass-spring model, which was developed based on condensation method applicable to ENM, and show that the model is able to accurately predict the fluctuation behavior of proteins. We applied this modified mass-spring model to analyze the conformational changes in proteins. We consider two model proteins as an example, where these two proteins exhibit different functions and molecular sizes. It is shown that the modified mass-spring model allows for accurately predicting the pathways of conformation changes for proteins. Our model provides structural insights into the conformation change of proteins related to the biological functions of large protein complexes.

Keywords: Mass-spring model, Condensation method, Normal mode analysis, Conformation change.

1. INTRODUCTION

A conformation change is a change in the structure of proteins that generally occurs during the biological function of the protein [1]. In general, this event is well captured by the low-frequency normal modes of proteins. An understanding of the conformational change in proteins leads us to gain insight into the biological function of the protein, the mechanism of disease occurrence in the human body, and to design drugs. In previous studies, two equilibrium states—open and closed states—have been used separately for understanding the dynamic behavior of protein related to biological function [2-8]. However, since the conformation change of protein is known to be significantly related to the molecular vibrations generated by thermal fluctuation, mechanical approaches have also been used to study protein conformations [9].

Low-frequency modes of protein conformation driven by thermal energy are analyzed by normal mode analyses (NMA), which enable interpretation of the intermediate conformations during the conformation change of protein. Molecular dynamics (MD) simulation is conventionally used for protein dynamics, but it is restricted to studying small proteins due to the limited time scales of MD simulations. In particular, the time scale accessible with MD simulation is much shorter than the time scale relevant for the conformational change of proteins, since it considers all atoms in a protein molecule and therefore has a high degree of freedom [10].

A simple mass-spring-based model called the elastic network model (ENM) was suggested by Tirion in 1996 [11]. ENM considers the α-carbon atoms in the backbone of the protein structure as the mass of the system [2,4]. Interactions between atoms are simplified to harmonic interactions, so that they are described as harmonic springs. ENM does not take into account

* Corresponding author (nass@korea.ac.kr)

DOI : 10.1017/jmech.2015.109
Copyright © 2015 The Society of Theoretical and Applied Mechanics, R.O.C.
https://doi.org/10.1017/jmech.2015.109 Published online by Cambridge University Press

the details of chemical interactions owing to its simplicity, but this simple mass-spring model has performed well in combination with NMA for calculating low-frequency modes of proteins [1,12,13].

ENM has been modified into several different types of analyses, which use different criteria in selecting the mass from the original structure, or applying other methods in combination with ENM, etc. The basic types of ENM are the Gaussian network model (GNM) [4] and the anisotropic network model (ANM) [2]. These are the original elastic models (for proteins), of which GNM is an isotropic one-dimensional model, while ANM is an anisotropic three-dimensional model. Since GNM is an isotropic model with an $N \times N$ (N: number of α-carbon atoms)-sized matrix system and ANM is an anisotropic model with a $3N \times 3N$-sized matrix system, computational cost of GNM is smaller than that of ANM. However in comparison with experimental results, the protein's dynamic behavior such as thermal fluctuation is described more accurately in GNM than in ANM. However, GNM is an isotropic one-dimensional model that assumes that the protein's dynamic behaviors in three directions (x-, y-, z-axes) are the same, and hence, it is not able to provide the three-dimensional motion of the protein. In contrast, conformational change is a three-dimensional structural change of the protein, which can be described by the normal modes of ANM. In particular, recent studies report that ANM allows for analysis of the structural change in proteins [14,15] and three-dimensional motions such as bending, torsion, and axial motion [16,17].

Recent improvements in technology have yielded structural information from experiments that show complete structures of large protein; this information is of particular interest since many large proteins are membrane proteins [18,19] Many large proteins are related to newly interested membrane proteins [18,19] or motor proteins [20]. Dealing with these large proteins is particularly challenging for simulation studies. Although ENM is computationally efficient for studying large protein dynamics when compared with all-atom models, it requires high computational cost to analyze larger structures [21]. To increase the efficiency of ENM, some modifications were applied to ENM [22,23]. Reducing the atom number of a structure has been the simplest way to increase the efficiency of calculating normal modes using ENM. A condensation method was applied to the ENM-based model, which we term "modified mass-spring model," to reduce the size of the system matrix by selecting master residues for calculation [7-9,24]. This method yielded effective calculations using computation resources, since the system size decreased whilst maintaining high correlations with original ENM analyses and experimental results of thermal fluctuations. In particular, the condensation method applied to GNM and ANM enables the computationally efficient analysis of large protein dynamics.

In this study, we applied the modified mass-spring model to simulate the intermediate states of protein undergoing a conformational change. Normal modes generated from the modified mass-spring model well simulated protein motions. By applying these modes to the initial structure, we generated intermediate states of the protein during the conformational change and found similar structures in bound form. We generated the structure in bound form and confirmed the simulation data using the root mean square deviation (RMSD), energy, and displacements obtained as the results. The robustness of the applied low-frequency normal modes using the modified mass-spring model with protein dynamics was confirmed by calculating overlap and showing the number of modes used for the conformational change in each iteration step.

2. METHODS

Conformational change in protein structures is simulated by a combination of different methods. In this section, the complete analysis procedure of the conformational change and each method used in the process are described separately.

2.1 Conformation Change Process

In this section, the conformation change process simulated by the present method is described. As described in Fig. 1, we started with the protein structure from the protein data bank (PDB) as the initial state of the protein for constructing the mass-spring model. We applied the condensation method to the original mass-spring model, reducing the size of the stiffness matrix and the mass matrix, and carried out NMA by solving the eigenvalue problem with the reduced matrices to obtain the normal modes of the initial structure. From 10 low-frequency normal modes, overlap with the direction vector (vector of atoms between the initial and final structures of protein) was calculated and the normal mode with the highest overlap was selected. With this selected low-frequency normal mode, the structure was changed by ±0.1 Å in all directions for energy calculations. Energy minimization was applied to both the generated structures to find the stable one, since the normal mode calculated using the condensation method has a smaller degree of freedom than the original structure. After energy minimization, the structure with the lower energy value was selected and the entire process was repeated until the final structure of the target protein was found by calculating the RMSD.

2.2 Elastic Network Model (ENM)

ENM was suggested by Tirion using an α-carbon-atom-based harmonic potential to describe atomic interactions of a protein structure (Tirion [11]; Haliloglu, Bahar and Erman [4]). Proteins are composed of different types of amino acids, each type having a different number of atoms. In an all-atom MD simulation or an all-atom NMA, these atoms are considered for constructing the protein structure and the degrees of freedom are larger than the total number of amino acids that constitute the protein. ENM considers the α-carbon atoms of amino acids that form the backbone of the polypeptide chain, so the degrees of freedom are reduced to the number of amino acids; hence, ENM needs a smaller space than all-atom models.

https://doi.org/10.1017/jmech.2015.109 Published online by Cambridge University Press

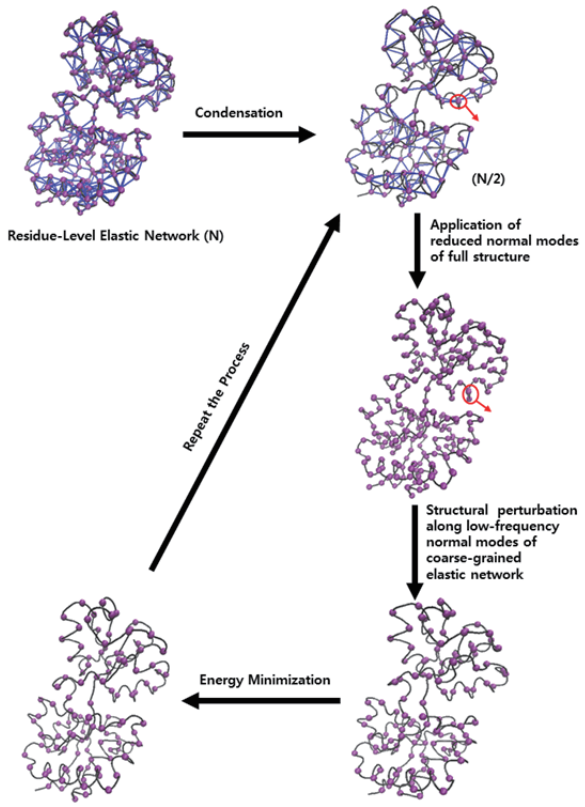


Fig. 1 Schematic of process for conformation change of protein with modified mass-spring model.

In all-atom models, the potential energy consists of various types of interactions that indicate the different interactions between various types of atoms. However, since ENM considers only one type of α-carbon atom, the interactions between atoms are also described by one potential, namely, the harmonic potential. The harmonic potential is applied to the protein structure, and a cut-off distance is used to define the range of interaction. Harmonic potential and the Hessian matrix after applying the cut-off distance are described by the following equation.

$$V = \frac{\gamma}{2}\sum_{i=1}^{N}\sum_{j\neq 1}^{N}\left[|\mathbf{r}_i-\mathbf{r}_j|-|\mathbf{r}_i^0-\mathbf{r}_j^0|\right]^2\cdot H\left(r_c-|\mathbf{r}_i^0-\mathbf{r}_j^0|\right) \quad (1)$$

Here, γ is a force constant that decides the strength of the interaction between the atoms of a protein, N is the number of residues (the number of α-carbon atoms), $\mathbf{r}_i$ is a coordinate of the i-th residue, r_c is the cut-off distance that decides the range of interaction, and H(x) is the Heaviside step function defined as $H(x) = 0$ if $x < 0$ (otherwise, $H(x) = 1$). The cut-off distance is set as 12 Å.

To calculate NMA, the stiffness (Hessian) matrix has to be computed from a potential field given by Eq. (1). The stiffness matrix **K** for ENM is composed of 3 × 3 block matrices $\mathbf{k}_{ij}$ given as

$$\mathbf{K} = \begin{bmatrix} \mathbf{k}_{11} & \mathbf{k}_{12} & \cdots & \mathbf{k}_{1N} \\ \mathbf{k}_{21} & & & \mathbf{k}_{2N} \\ \vdots & & & \vdots \\ \mathbf{k}_{N1} & \mathbf{k}_{N2} & \cdots & \mathbf{k}_{NN} \end{bmatrix} \quad (2)$$

The ijth elements (i ≠ j) $\mathbf{k}_{ij}$ of **K** is given by

$$\mathbf{k}_{ij} = \begin{bmatrix} \frac{\partial^2 V}{\partial X_i \partial X_j} & \frac{\partial^2 V}{\partial X_i \partial Y_j} & \frac{\partial^2 V}{\partial X_i \partial Z_j} \\ \frac{\partial^2 V}{\partial Y_i \partial X_j} & \frac{\partial^2 V}{\partial Y_i \partial Y_j} & \frac{\partial^2 V}{\partial Y_i \partial Z_j} \\ \frac{\partial^2 V}{\partial Z_i \partial X_j} & \frac{\partial^2 V}{\partial Z_i \partial Y_j} & \frac{\partial^2 V}{\partial Z_i \partial Z_j} \end{bmatrix} \quad (3)$$

The equation of motion for protein dynamics described under harmonic approximation is $\mathbf{M}(d^2\mathbf{R}/dt^2) + \mathbf{KR} = 0$, where **M** is the mass matrix for α-carbon atoms (a diagonal matrix), **R** is a column vector representing the atomic coordinates of α-carbon atoms, *i.e.*, $\mathbf{R}^\dagger = [\mathbf{r}_1^\dagger, \mathbf{r}_1^\dagger, \ldots, \mathbf{r}_N^\dagger]$, and **K** is the stiffness matrix composed of block matrices $\mathbf{k}_{ij}$ given by Eq. (3). For vibration of the protein structure, the atomic coordinates **R** were assumed as $\mathbf{R} = \mathbf{u}\exp[i\omega t]$, where ω is the natural frequency and **u** is its corresponding normal mode. Under the assumption of $\mathbf{M} = m\mathbf{I}$, where m is the molecular weight of α-carbon atoms and **I** is the $3N \times 3N$ diagonal matrix, the equation of motion becomes the eigenvalue problem: $\mathbf{Ku} = \omega^2 m\mathbf{u} = \lambda\mathbf{u}$, where λ is the eigenvalue.

2.3 Modified Mass-Spring Model

The condensation method enables coarse-graining of protein structures with smaller numbers of residues, which is known as the modified mass-spring model [8,9]. We consider (N/n) residues, referred to as master residues, for the coarse-grained structure. The remaining $N(1-1/n)$ residues, referred to as slave residues, are removed during coarse-graining. Partitioning the master and slave residues, we can express the potential energy as follows:

$$V = \frac{1}{2}\mathbf{u}^\dagger\mathbf{K}\mathbf{u} = \frac{1}{2}[\mathbf{u}_\alpha^\dagger\mathbf{u}_\beta^\dagger]\begin{bmatrix}\mathbf{K}_{\alpha\alpha} & \mathbf{K}_{\alpha\beta} \\ \mathbf{K}_{\beta\alpha} & \mathbf{K}_{\beta\beta}\end{bmatrix}\begin{bmatrix}\mathbf{u}_\alpha \\ \mathbf{u}_\beta\end{bmatrix} \quad (4)$$

Here, the Greek symbols α and β denote the master and slave residues, respectively.

Following the condensation method, the reduced stiffness matrix for the modified mass-spring model is given by

$$\mathbf{K}_1 = \mathbf{K}_{\alpha\alpha} - \mathbf{K}_{\alpha\beta}\mathbf{K}_{\beta\beta}^{-1}\mathbf{K}_{\beta\alpha} \quad (5)$$

In addition, the reduced mass matrix for the modified mass-spring model can be represented in the form $\mathbf{M}_1 = m\mathbf{I}_\alpha$, where m is the molecular weight of an α-carbon atom and $\mathbf{I}_\alpha$ denotes a $3(N/n) \times 3(N/n)$ identity matrix, where N is the total number of α-carbon atoms and n is the degree of condensation.

https://doi.org/10.1017/jmech.2015.109 Published online by Cambridge University Press

From Eq. (5), $\mathbf{M}_1$, the fluctuation dynamics of the modified mass-spring model composed of master residues, is described as

$$\mathbf{K}_1\mathbf{u}_1 = \omega^2 m\mathbf{u}_1 \tag{6}$$

where $\mathbf{u}_1$ is the normal mode of the modified mass-spring model.

2.4 Generating New Conformation

Reduced normal modes are applied to the protein structure to find the pathways of conformational change. A single low-frequency normal mode is selected to perturb the structure, and the overlap between the direction vector and the 10 low-frequency normal modes is calculated. The overlap for the *j*-th normal mode is shown as follows:

$$O_j = \frac{\left|\sum^{3N}\mathbf{u}_{1ij}\Delta\mathbf{r}_i\right|}{\left[\sum^{3N}\mathbf{u}_{1ij}^2\sum^{3N}\Delta\mathbf{r}_i^2\right]^{1/2}} \tag{7}$$

where $\Delta\mathbf{r}_i = \mathbf{r}_i^o - \mathbf{r}_i^c$; and $\mathbf{r}_i^o$ and $\mathbf{r}_i^c$ are the *i*-th atomic coordinates of the open and closed structures, respectively. From the 10 low-frequency normal modes, one single mode that gives the highest correlation value is chosen.

Intermediate structures with the selected low-frequency normal modes are generated as follows:

$$\mathbf{R}_{new} = \mathbf{R} \pm \mathbf{u}_{1j} \times DF \tag{8}$$

where $\mathbf{R}_{new}$ denotes the new position vector of the protein structure, $\mathbf{R}$ is the position vector of the protein structure before the perturbation, and *DF* is a deformation factor that defines the amplitude of structural change (*DF* = 0.1 Å). Two structures are generated from the low-frequency normal modes to find an energetically stable conformation.

2.5 Energy Minimization

Since two new conformations $\mathbf{R}_{new}^+$ and $\mathbf{R}_{new}^-$ are generated using the reduced normal modes, the two α-carbon backbone atoms are deformed along the same normal mode direction. These deformed conformations are relaxed by applying energy minimization, and an energetically stable conformation is found for each direction. For energy minimization, the steepest descent method is applied with 40000 steps for every iteration of the conformation change process of each model protein. The Gō-potential is used as the potential energy for energy minimization. The Gō-potential is built by contact bonds and native (noncontact) bonds and used for protein folding problems. After energy minimization, the energies of the two conformations $\mathbf{R}_{new}^+$ and $\mathbf{R}_{new}^-$ are compared, and the conformation with the lower energy, which is the more stable conformation, is chosen.

3. RESULTS AND DISCUSSIONS

Adenylate kinase and T4 phage beta-glucosyltransferase were used as model proteins for simulation and verification of the conformational change in biomolecules by using the mechanical modified mass-spring model, which generates intermediate states during the conformational change. The experimental data of these proteins deposited in the protein data bank (www.pdb.org) were employed. In particular, the PDB codes of both the open and closed forms exist on the database for adenylate kinase (open: 4AKE, close: 1AKE) and for T4 phage beta-glucosyltransferase (open: 1JEJ, close: 1JG6), which are taken into account in our conformational change simulations. These two selected models perform different functions in nature and show dissimilar conformational changes, which will serve to establish the robustness of the normal modes calculated from the modified mass-spring model in combination with the condensation method. Verification of the protein structure with the modified mass-spring model has been performed in our previous studies using various parameters such as B-factor comparison and normal mode comparison, which are related to the thermal fluctuation of proteins [5,7-9]. Previous studies have shown that condensation method describes thermal fluctuation behaviors of protein very well. Not just the fluctuation behaviors but the importance of low-frequency normal modes on protein dynamics were shown using condensation methods. Therefore, in this study, the conformational change was simulated using the modified mass-spring model, without verification of the modified mass-spring model.

In Fig. 2, the open form (left), closed form (middle), and the form predicted using the method described herein (right) are shown for adenylate kinase (Fig. 2(a)) and T4 phage beta-glucosyltransferase (Fig. 2(b)). Adenylate kinase binds to the ligand by changing two domains of its structure: The LID domain (residues 122-158) and the AMP-binding domain (residues 30-63) (red parts in figure). These two domains show significant differences in the open-form structure 4AKE (left) and the closed-form structure 1AKE (middle) and are closed in the closed form of the structure. The predicted form shown on the right shows the movement of the two domains during the closing motion. T4 phage beta-glucosyltransferase is a DNA binding protein, and therefore, the conformational change in its structure is related to binding DNA and the major movement is made by the C-terminal domain (residues 184-351, red parts in the figure). The open-form structure 1JEJ and the closed-form structure 1JG6 show differences in the C-terminal domain, which undergoes a closing motion with respect to the other parts colored gray. The form predicted by our simulation (on the right) shows the movements of the C-terminal domain during the closing motion, which is the major conformational change.

The structural change is generally measured by RMSD and is that occurring during time steps or iteration steps. First, the RMSD between the open and

https://doi.org/10.1017/jmech.2015.109 Published online by Cambridge University Press

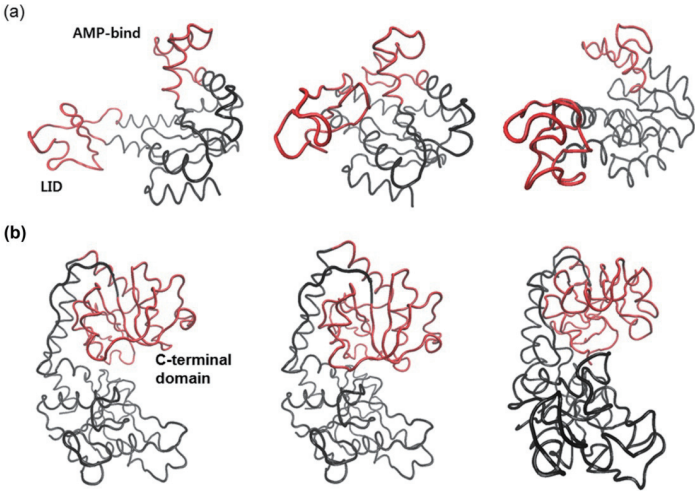


Fig. 2 (a) Structure of Adenylate Kinase in open form (left), close form (middle), and predicted close form with our method (right). Two domains which show major conformation change, AMP-binding domain and LID domain are colored in red. (b) Structure of T4 phate beta-glucosyltransferase in open form (left), close form (middle), and predicted close form with our method (right). The C-terminal domain which shows structural change is colored in red.

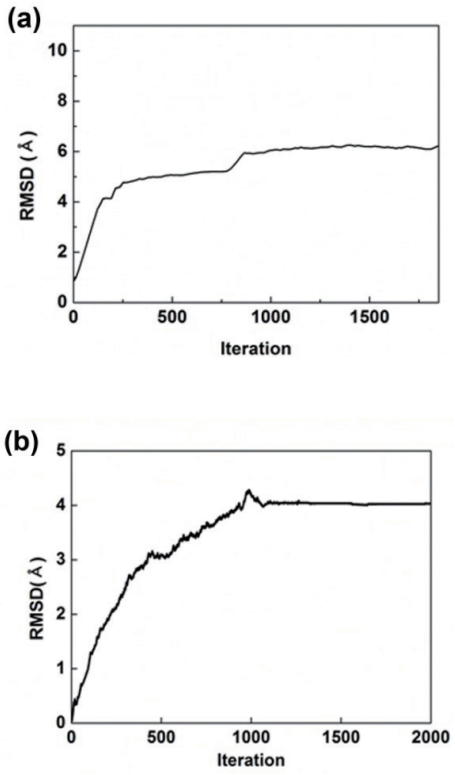


Fig. 3 RMSD measurement of (a) Adenylate Kinase and (b) T4 phage beta-glucosyltransferase.

closed forms of each model protein is measured to formulate guidelines for the conformational change. Structural position data of these two conformations are obtained from PDB, which are the results from experiments conducted with real proteins. Therefore, measuring the RMSD between these two conformations provides a realistic measurement of the structural differences in the two model proteins during the conformational change. The RMSD value of adenylate kinase is measured as 6.9 Å, and that of the T4 phage beta-glucosyltransferase is 4.5 Å. Figure 3 depicts the RMSD values with respect to the iteration number of the two models during conformation change. The RMSD is an index that identifies the completion of the conformational change and the stabilization of the structure. The RMSD plot of adenylate kinase shown in Fig. 3(a) indicates two steps of structural change during the conformational change. The RMSD increases rapidly in ~200 steps and stabilizes at around 5 Å in ~900 steps, and then increases slightly up to 6.2 Å and subsequently stabilizes by the end of the simulation. Figure 3(b) shows the RMSD plot of the T4 phage beta-glucosyltransferase, and it steadily increases until ~1100 steps and stabilizes at 4.2 Å at the final step of the simulation. The two protein models show different RMSD change behaviors, *i.e.*, a two-step change for adenylate kinase and a one-step change for the T4 phage beta-glucosyltransferase during the simulation of the conformational change. It is speculated that because of the structural characteristics of the conformational change, adenylate kinase changes two domains in its structure and the T4 phage beta-glucosyltransferase changes only one domain in its structure.

Residue displacements between open and closed forms (experimental structures) of model proteins are calculated, and the open and predicted structures are used to compare the behaviors of structural movements. Displacements of adenylate kinase and the T4 phage beta-glucosyltransferase are shown in Fig. 4(a) and Fig. 4(b), respectively. As shown in Fig. 4, adenylate kinase shows major conformational changes in the LID domain (residues 122-158) and the AMP-binding (residues 30-63) domain, and also shows that these two domains undergo larger displacement changes than other parts and that the displacement measurement in the predicted structure (red line) follows the displacement behavior of the PDB structures. The T4 phage beta-glucosyltransferase shows a significant structural change in the C-terminal domain (residues 184-351), but not in all the other parts. In particular, the short linker (residues 169-183) and the α12helix (residues 317-335) that work as a linker of the C-terminal domain show smaller movements. Our simulation results show that the C-terminal domain undergoes more structural changes than the other domains of the model protein. However, displacement measurements obtained by the simulations show larger changes than those obtained experimentally. The displacement measurements show that the C-terminal domain of the T4 phage beta-glucosyltransferase has a relatively larger displacement change than the other domains, similar to the experiment results. The results in Fig. 4(b) also show the same behavior of movement of the C-terminal domain.

https://doi.org/10.1017/jmech.2015.109 Published online by Cambridge University Press

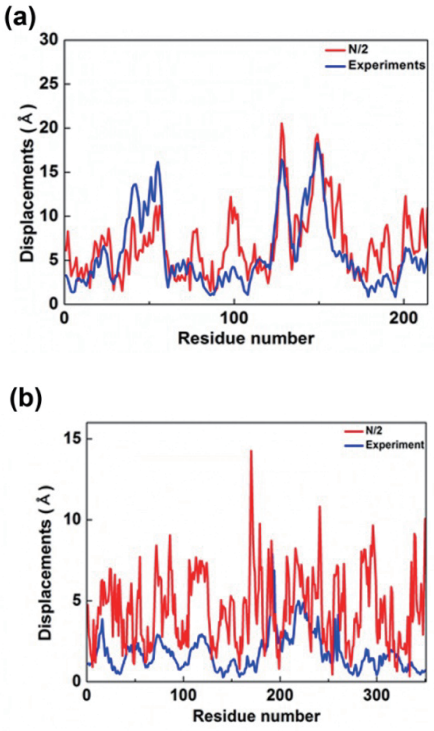


Fig. 4 Residue displacement measurement of (a) Adenylate Kinase for simulation (Red) and experiment (Blue), (b) T4 phage beta-glucosyl transferase for simulation (Red) and experiment (blue).

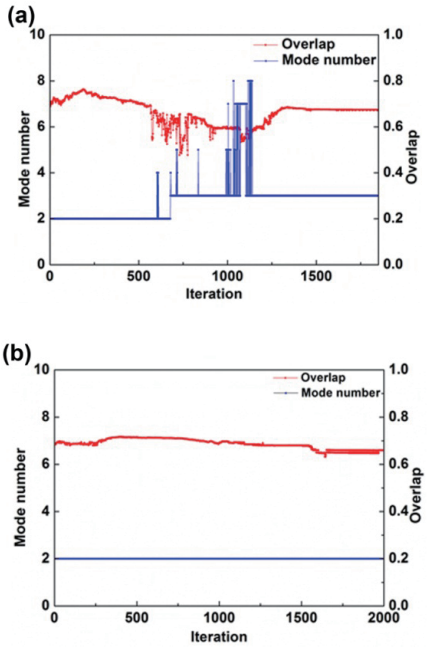


Fig. 5 Overlap between low-frequency normal mode and direction vector (red) and selected mode number (blue) of (a) adenylate kinase shows major two modes (2nd and 3rd) used for conformation change in the major structural change in two domains and (b) T4 phage beta-glucosyltransferase shows one low-frequency normal mode (2nd) used for conformation change in one domain.

To verify the reliability of the reduced normal mode used for conformation change, the overlap value with the direction vectors of the open and closed forms of the model protein was calculated and the mode number of the selected normal mode was found. Figures 5(a) and 5(b) show overlap results following iteration steps and the selected mode number for each iteration step of adenylate kinase and the T4 phage beta-glucosyltransferase, respectively. The overlap value of adenylate kinase is ~0.7 in 0-500 steps and reduces to ~0.6 at 500-1000 steps; it then increases after 1200 steps. This behavior is related to the change in the dominant normal mode, selected for conformation change by the correlation value. The structural deformation in adenylate kinase follows from the 2nd and 3rd low-frequency normal modes calculated from the modified mass-spring model and agrees with the trend of the structural change. The results show that the modified mass-spring model well reproduces the structural change of adenylate kinase following the mode numbers. Figure 5(b) also shows the results for the T4 phage beta-glucosyltransferase, indicating that overlap is maintained steadily at > 0.65 and the structural change follows the 2nd low-frequency normal mode. Since the T4 phage beta-glucosyltransferase shows only a one-sided structural change, the large structural deformation can be explained by a single mode, *i.e.*, the 2nd low-frequency normal mode from the modified mass-spring model; further, and the modified mass-spring model agrees well with the original mass-spring model in describing the conformational change using the 2nd low-frequency normal mode for the entire process. The conformation change process predicted by the modified mass-spring model showed results consistent with the characteristic of the protein structures found in experiments and the original mass-spring model during its structural deformation.

4. CONCLUSIONS

This research describes the process for simulating the conformation change of protein using a modified mass-spring model. The conformation change process of a protein can be described by protein dynamics, and thermal vibrations with NMA. In this work, we applied the modified mass-spring model, which describes protein dynamics, using smaller degrees of freedom than the original mass-spring model, and our method increased the computational efficiency in terms of memory and calculation time about 25%. The RMSD results show stabilization of the structure at the end of conformational change process, and the energy values are also stabilized with RMSD by decreasing in the final states when a closed form is generated. The displacement results follow the structural change tendency of the experimental results, where adenylate kinase showed greater movements in the LID domain and the AMP-binding domain and the T4 phage beta-glucosyltransferase showed relatively more structural change in the C-terminal domain. The low-frequency normal modes selected for conformation change

https://doi.org/10.1017/jmech.2015.109 Published online by Cambridge University Press

showed the same behavior as the original mass-spring model with the same index of selected normal modes and adenylate kinase showed two major low-frequency normal modes for conformation change for the structural change of each domain. Only one low-frequency normal mode was selected for the T4 phage beta-glucosyltransferase for the entire process, which shows a structural change in only one domain. The modified mass-spring model well reproduced the structural changes of the two model proteins with reduced low-frequency normal modes, in accordance with the behavior observed in the experiments and understood by the mass-spring model. Our model is computationally effective in determining the conformation change pathway with large structural deformations and it may be useful in predicting the pathways of protein structures whose one conformation is only known.

ACKNOWLEDGEMENTS

This research was supported by National Research Foundation of Korea (NRF) under Grant No. NRF-2015-R1A2A2A04002453, and the Korea Institute of Science and Technology Information (KISTI) under Grant No. KSC-2015-C3-031 (to K.E.), and NRF under Grant (No.2007-0056094) and (No.2014R1A2A1A11052389) (to S.N.).

REFERENCES

1. Bahar, I. and Rader, A. J., "Coarse-Grained Normal Mode Analysis in Structural Biology," *Current Opinion in Structural Biology*, **15**, pp. 586–592 (2005).
2. Atilgan, A. R., *et al*., "Anisotropy of Fluctuation Dynamics of Proteins with an Elastic Network Model," *Biophysical Journal*, **80**, pp. 505–515 (2001).
3. Bahar, I., *et al*., "Vibrational Dynamics of Folded Proteins: Significance of Slow and Fast Motions in Relation to Function and Stability," *Physical Review Letters*, **80**, p. 2733 (1998).
4. Haliloglu, T., Bahar, I. and Erman, B., "Gaussian Dynamics of Folded Proteins," *Physical Review Letters*, **79**, p. 3090 (1997).
5. Kim, J. I., Na, S. and Eom, K., "Domain Decomposition-Based Structural Condensation of Large Protein Structures for Understanding Their Conformational Dynamics," *Journal of Computational Chemistry*, **32**, pp. 161–169 (2011).
6. Kim, J.-I., Na, S. and Eom, K., "Large Protein Dynamics Described by Hierarchical-Component Mode Synthesis," *Journal of Chemical Theory and Computation*, **5**, pp. 1931–1939 (2009).
7. Kim, J. I., *et al*., "A 3-D Coarser-Grained Computational Model for Simulating Large Protein Dynamics. Computers," *Materials & Continua*, **9**, pp. 137–152 (2009).
8. Eom, K., *et al*., "Coarse-Graining of Protein Structures for the Normal Mode Studies," *Journal of Computational Chemistry*, **28**, pp. 1400–1410 (2007).
9. Eom, K., *et al*., "Modified Mechanical Mass-Spring Model of Biomolecules for Understanding Dynamics of Proteins," *Journal of Mechanical Science and Technology*, **22**, pp. 506–513 (2008).
10. Cui, Q. and Bahar, I., *Normal Mode Analysis: Theory and Applications to Biological and Chemical Systems*, Chapman & Hall/CRC, U.K (2006).
11. Tirion, M. M., "Large Amplitude Elastic Motions in Proteins from a Single-Parameter," *Atomic Analysis. Physical Review Letters*, **77**, p. 1905 (1996).
12. Maragakis, P. and Karplus, M., "Large Amplitude Conformational Change in Proteins Explored with a Plastic Network Model: Adenylate Kinase," *Journal of Molecular Biology*, **352**, pp. 807–822 (2005).
13. Li, G. and Cui, Q., "A Coarse-Grained Normal Mode Approach for Macromolecules: An Efficient Implementation and Application to Ca^{2+}-ATPase," *Biophysical Journal*, **83**, pp. 2457–2474 (2002).
14. Kim, M. K., Jernigan, R. L. and Chirikjian, G. S., "Efficient Generation of Feasible Pathways for Protein Conformational Transitions," *Biophysical Journal*, **83**, pp. 1620–1630 (2002).
15. Kantarci-Carsibasi, N., Haliloglu, T. and Doruker, P., "Conformational Transition Pathways Explored by Monte Carlo Simulation Integrated with Collective Modes," *Biophysical Journal*, **95**, pp. 5862–5873 (2008).
16. Yoon, G., *et al*., "Mechanical Characterization of Amyloid Fibrils Using Coarse-Grained Normal Mode Analysis," *Advanced Functional Materials*, **21**, pp. 3454–3463 (2011).
17. Ming, D., *et al*., "Substructure Synthesis Method for Simulating Large Molecular Complexes," *Proceedings of the National Academy of Sciences*, **100**, pp. 104–109 (2003).
18. Xiong, J.-P., *et al*., "Crystal Structure of the Extracellular Segment of Integrin Alpha Vbeta 3," *Science*, **294**, pp. 339–345 (2001).
19. Xiong, J.-P., *et al*., "Crystal Structure of the Extracellular Segment of Integrin alpha Vbeta 3 in Complex with an Arg-Gly-Asp Ligand," *Science*, **296**, pp. 151–155 (2002).
20. Ranson, N. A., *et al*., "ATP-Bound States of GroEL Captured by Cryo-Electron Microscopy," *Cell*, **107**, pp. 869–879 (2001).
21. Tozzini, V., "Coarse-Grained Models for Proteins," *Current Opinion in Structural Biology*, **15**, pp. 144–150 (2005).
22. Jang, H., Na, S. and Eom, K., "Multiscale Network Model for Large Protein Dynamics," *The Journal of Chemical Physics*, **131**, pp. 245106–2451010 (2009).
23. Kim, M. K., Jernigan, R. L. and Chirikjian, G. S., "Rigid-Cluster Models of Conformational Transitions in Macromolecular Machines and Assemblies," *Biophysical Journal*, **89**, pp. 43–55 (2005).
24. Eom, K., *et al*., "Robust Reduction Method for Biomolecules Modeling," *CMC-Computers Materials & Continua*, **6,** pp. 35–42 (2007).

(Manuscript received September 4, 2013,
accepted for publication October 16, 2015.)

https://doi.org/10.1017/jmech.2015.109 Published online by Cambridge University Press